Taylor & Francis
Taylor & Francis Group

ORIGINAL RESEARCH

Check for updates

M7824, a novel bifunctional anti-PD-L1/TGFβ Trap fusion protein, promotes anti-tumor efficacy as monotherapy and in combination with vaccine

Karin M. Knudson[a], Kristin C. Hicks[a], Xiaoling Luo[b], Jin-Qiu Chen[b], Jeffrey Schlom[a,†], and Sofia R. Gameiro[a,†]

[a]Laboratory of Tumor Immunology and Biology, Center for Cancer Research, National Cancer Institute, National Institutes of Health, Bethesda, MD, USA; [b]Collaborative Protein Technology Resource (CPTR), Center for Cancer Research, National Cancer Institute, National Institutes of Health, Bethesda, MD, USA

ABSTRACT

Tumors evade host immune surveillance through multiple mechanisms, including the generation of a tumor microenvironment that suppresses immune effector function. Secretion of TGFβ and upregulation of immune checkpoint programmed cell death ligand-1 (PD-L1) are two main contributors to immune evasion and tumor progression. Here, we examined the efficacy of a first-in-class bifunctional checkpoint inhibitor, the fusion protein M7824, comprising the extracellular domain of human TGFβRII (TGFβ Trap) linked to the C-terminus of human anti-PD-L1 heavy chain (αPD-L1). We demonstrate that M7824 reduces plasma TGFβ1, binds to PD-L1 in the tumor, and decreases TGFβ-induced signaling in the tumor microenvironment in mice. In murine breast and colon carcinoma models, M7824 decreased tumor burden and increased overall survival as compared to targeting TGFβ alone. M7824 treatment promoted CD8+ T cell and NK cell activation, and both of these immune populations were required for optimal M7824-mediated tumor control. M7824 was superior to TGFβ- or αPD-L1-targeted therapies when in combination with a therapeutic cancer vaccine. These findings demonstrate the value of using M7824 to simultaneously target TGFβ and PD-L1/PD-1 immunosuppressive pathways to promote anti-tumor responses and efficacy. The studies also support the potential clinical use of M7824 as a monotherapy or in combination with other immunotherapies, such as therapeutic cancer vaccines, including for patients who have progressed on αPD-L1/αPD-1 checkpoint blockade therapies.

Introduction

In recent years, therapeutics targeting the immune system have become a major treatment modality in cancer. Monoclonal antibodies targeting immune checkpoints, such as programmed cell death-1 (PD-1) and programmed cell death ligand-1 (PD-L1), are a major class of these agents. The PD-1 receptor is expressed on activated T and natural killer (NK) cells. After interaction with its ligands PD-L1 and PD-L2, which are typically expressed on antigen presenting cells, PD-1 regulates immune responses by inhibiting T and NK cell maturation, proliferation, and effector function.[1,2] Aberrant overexpression of PD-L1 has been observed in numerous malignancies and is associated with poor clinical outcome.[3,4] Antibodies blocking PD-L1 or PD-1 inhibit this immunosuppressive pathway and have led to improvements in patient survival in melanoma,[5,6] lung cancer,[7,8] bladder cancer,[9,10] and Merkel cell carcinoma,[11,12] among others.[2] Avelumab, which targets PD-L1, is approved for use in Merkel cell carcinoma and urothelial carcinoma. However, for most solid tumor types excluding melanoma, only 10–20% of patients typically respond to PD-1/PD-L1-targeted therapies.[2] Therefore, improvement of these therapeutics is needed to increase patient response and survival.

In addition to expression of immune checkpoints, the tumor microenvironment (TME) contains other immunosuppressive molecules. Of particular interest is the cytokine TGFβ, which has multiple functions in cancer. TGFβ prevents proliferation and promotes differentiation and apoptosis of tumor cells early in tumor development. However, during tumor progression, tumor TGFβ insensitivity arises due to the loss of TGFβ receptor expression or mutation to downstream signaling elements. TGFβ then promotes tumor progression through its effects on angiogenesis, induction of epithelial-to-mesenchymal transition (EMT), and immune suppression.[13,14] TGFβ mediates immune suppression by preventing the activation and division of T cells and decreasing effector function of both T and NK cells.[13,15] In addition, TGFβ can induce the differentiation of regulatory CD4+ T cells (T_reg),[16,17] an indicator of poor prognosis for many tumor types.[18,19] High TGFβ serum level and loss of TGFβ receptor (TGFβR) expression on tumors correlates with poor prognosis,[20-22] which makes this pathway a noteworthy target for novel therapeutics.[23,24] TGFβ-targeted therapies have demonstrated limited clinical activity. To our knowledge, however, none have targeted TGFβ inhibition

or sequestration in the TME. TGFβ is a pleotropic cytokine involved in normal physiological function, which may be why small molecule inhibitors targeting TGFβ-dependent signaling have shown a high propensity for associated toxicities in preclinical models, including cardiac toxicities and the development of neoplasms.[23]

PD-L1 and TGFβ regulate immune suppression in the TME in distinct yet complementary ways. It is possible that targeting both the PD-L1 and TGFβ negative regulatory pathways simultaneously will increase anti-tumor efficacy. Here, we utilized a first-in-class bifunctional fusion protein designed to block PD-L1 and sequester TGFβ in the TME. M7824 (MSB0011395C) comprises the extracellular domain of human TGFβ receptor II (TGFβRII) linked to the C-terminus of the human αPD-L1 heavy chain, based on the human IgG1 monoclonal antibody (mAb) avelumab.[25] To evaluate the PD-L1 versus TGFβ-targeted modes of action, we have also employed an M7824 mutant molecule devoid of the PD-L1 binding site. In this study, we evaluate the mechanisms of action and anti-tumor efficacy of M7824 in multiple murine tumor models and in combination with a therapeutic cancer vaccine.

Results

M7824 binds murine tumor PD-L1 in vitro and in vivo

M7824 is a fully humanized molecule, so we first determined whether M7824 binds to murine PD-L1. A dose dependent loss of detectable surface PD-L1 expression was observed on EMT6 breast carcinoma cells after treatment with M7824, indicating its ability to specifically bind surface PD-L1 and with an affinity similar to that of avelumab, a fully humanized mAb targeting PD-L1 (hereafter referred to as αPD-L1) (Fig. 1A). The functional PD-L1 binding domain on M7824 was required for PD-L1 binding, as indicated by the use of a control comprising human TGFβRII bound to a mutated αPD-L1 moiety (referred to as M7824mut or MUT), which did not bind to PD-L1 (Fig. 1A). Similar results were seen using 4T1 breast and MC38 colon carcinoma cell lines (Supplementary Figure 1A). M7824 also bound to murine PD-L1 expressed in the TME on CD45-negative cells in vivo as indicated by the loss of surface PD-L1 staining. The functional anti-PD-L1 moiety was required for M7824 binding to TME-expressed PD-L1 as indicated by similar surface PD-L1 staining between M7824mut and PBS treatment (Fig. 1B, left panel). Direct detection of M7824 was performed using an anti-human antibody that specifically binds human IgG heavy and light chain. The functional αPD-L1 moiety was required for M7824 to accumulate in the TME, as M7824mut was detected at low levels in the tumor (Fig. 1B, right panel). Thus, M7824 is able to specifically bind PD-L1 both in vitro and in vivo and deliver TGFβ Trap to the site of the tumor.

M7824 decreases tumor TGFβ signaling in vitro and in vivo and reduces plasma TGFβ1

There are three human and murine TGFβ isoforms, TGFβ1, TGFβ2, and TGFβ3. Binding of active TGFβ to the TGFβRI/TGFβRII receptor complex leads to phosphorylation and activation of canonical signaling molecules SMAD2 and SMAD3.[26] To examine the ability of M7824 to sequester murine TGFβ and

reduce TGFβ-dependent signaling, 4T1-pSMAD2-luc tumor cells, which express PD-L1 and TGFβRII and have intact TGFβ-dependent SMAD2/3 signaling (Supplementary Figure 1B, C), were used. Treatment of 4T1-pSMAD-luc tumor cells with M7824 either prior to (Fig. 1C) or after (Fig. 1D) the addition of TGFβ1 reduced TGFβ1-dependent phosphorylation of SMAD2, as indicated by decreased SMAD2 promoter-dependent luciferase activity (Fig. 1C, D). This effect was dependent on the TGFβ Trap portion of M7824, as M7824mut also reduced TGFβ-dependent signaling but αPD-L1 did not (Fig. 1C, D).

Treatment of EMT6 tumor-bearing mice with M7824 and M7824mut significantly reduced plasma levels of TGFβ1 after treatment (Fig. 1E), indicating their ability to bind to murine TGFβ1 in vivo. Plasma TGFβ2 and TGFβ3 levels were too low to detect in these studies. Importantly, M7824 also reduced intratumoral TGFβ signaling. Phosphorylation of SMAD2 in EMT6 tumors was significantly decreased 6 hours after M7824 treatment (Fig. 1F). Correlating with earlier results showing that M7824mut does not accumulate in the tumor (Fig. 1B), M7824mut did not reduce intratumoral SMAD2 signaling (Fig. 1F). M7824 treatment did not affect the phosphorylation of SMAD3 (Fig. 1F) or SMAD1 and SMAD5 (Supplementary Figure 1D) or activation of the non-canonical TGFβ-dependent signaling pathways ERK, JNK, or p38 (data not shown). These results support that M7824 sequesters murine TGFβ1 in vitro and in vivo. In addition, M7824 can both prevent the initiation of and significantly decrease existing TGFβ signaling, particularly in the TME.

M7824 promotes activation of CD8+ T cells and NK cells in non-tumor-bearing mice

TGFβ and PD-L1 affect T and NK cell phenotype and responses.[27,28] In order to determine the direct effect of M7824 on immune cell populations, we first examined their phenotype in the spleen and lymph nodes of non-tumor-bearing mice after M7824 treatment. M7824 treatment increased total cell numbers in the spleen (Fig. 2A, upper panel) but did not affect splenic CD8+ T cell (Fig. 2B, upper panel) or NK cell (Fig. 2F, upper panel) numbers. In contrast, total cell (Fig. 2A, lower panel), CD8+ T cell (Fig. 2B, lower panel), and NK cell (Fig. 2F, lower panel) numbers increased significantly in the lymph nodes. Frequencies of CD8+ T cells (Fig. 2C) and NK cells (Fig. 2G) did not significantly increase in either the spleen or lymph nodes. A greater proportion of both CD8+ T cell (Fig. 2D, upper panel) and NK cell (Fig. 2H, upper panel) populations displayed an activated, CD69+ phenotype in the spleen. In addition, M7824 treatment increased the frequency of splenic CD8+ T cells (Fig. 2D, lower panel) and NK cells (Fig. 2H, lower panel) entering the cell cycle, as indicated by Ki67 expression. The frequency of splenic activated CD44hi CD8+ T cells, specifically those with an effector or effector memory (T_{eff}/T_{EM}) CD44hiCD62Llo phenotype, was enhanced upon M7824 treatment (Fig. 2E). Total CD4+ T cell numbers, but not frequencies, significantly increased in the lymph nodes of M7824-treated mice (Supplementary Figure 2A). CD4+ T_{reg} numbers also increased in both spleen and lymph nodes (Supplementary Figure 2B). In contrast to the changes seen with
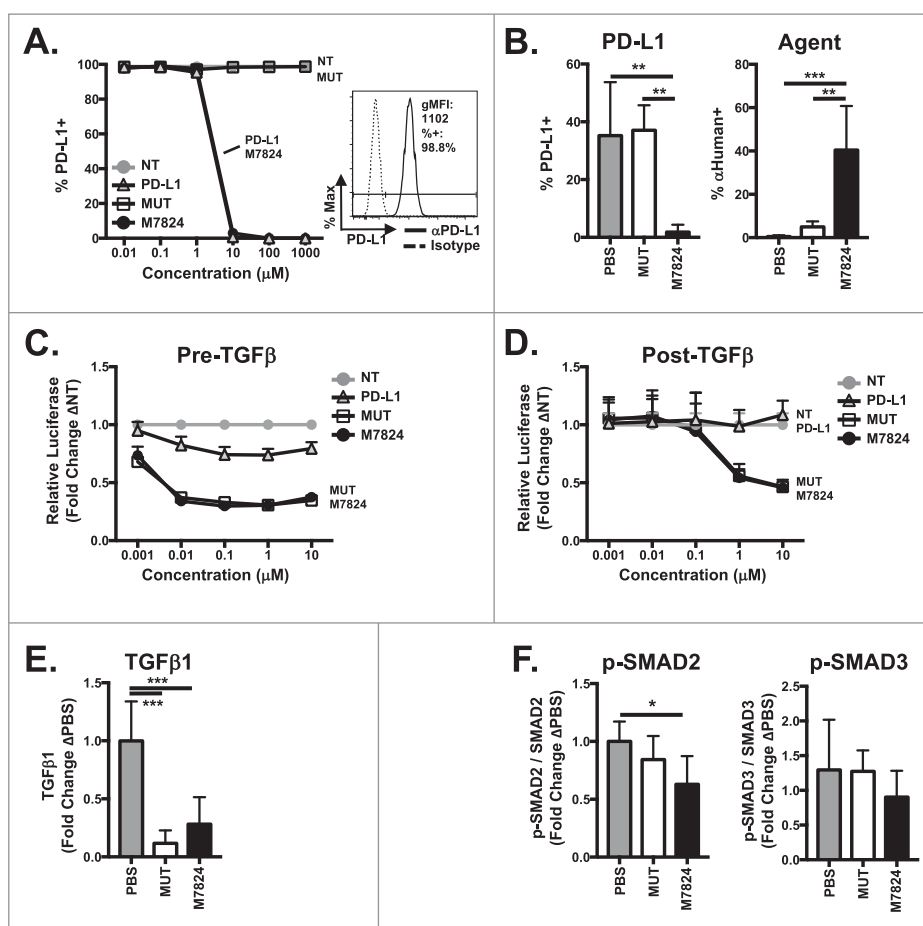
Figure 1. M7824 binds to murine PD-L1 and suppresses murine TGFβ signaling. (A) EMT6 tumor cells were treated with IFNγ for 24 hours to induce maximal PD-L1 expression (inset) followed by treatment with nothing (no treatment-NT), αPD-L1 (PD-L1), M7824mut (MUT), or M7824 for 30 minutes prior to analysis of surface PD-L1 expression by flow cytometry. Data represent 3 independent experiments. (B) 2.5×10^5 EMT6 tumor cells were orthotopically implanted into Balb/c mice. When tumor volumes reached 50–100mm^3, mice were treated i.p. at days 10, 12, and 14 with PBS or 492μg MUT or M7824. Twenty-four hours after the last treatment, intratumoral analysis of surface PD-L1 expression (left) and presence of biologic agents M7824mut or M7824 (right) on CD45 negative cells was performed by flow cytometry. Graphs show mean ± SD. Data represent 2 independent experiments, n = 5 mice. (C) 4T1-pSMAD2-luc tumor cells were exposed to PD-L1, MUT, or M7824 for 30 minutes followed by 2.5 ng/ml TGFβ1. Graph (mean ± SD) shows luciferase activity of SMAD2 reporter after 1 hour. Data represent 2 independent experiments. (D) 4T1-pSMAD2-luc tumor cells were treated with 2.5 ng/ml TGFβ1 for 30 minutes followed by PD-L1, MUT, or M7824. Graph (mean ± SD) shows luciferase activity of SMAD2 reporter after 6 hours. Data represent 3 independent experiments. (E) EMT6 tumor-bearing mice were treated as in (B). Twenty-four hours after the last treatment, plasma TGFβ1 level was examined. Graph shows mean ± SD. Data combined from 2 independent experiments, n = 3-6 mice per experiment. (F) EMT6 tumor cells were implanted as in (B). When tumor volumes reached 500mm^3, mice were treated at days 17, 19, and 21 with MUT or M7824. Six hours after the last treatment, phosphorylation and total level of SMAD2 and SMAD3 were determined by capillary Western blot. Graphs show mean ± SD. Data combined from 2 independent experiments, n = 2-5 mice per experiment.

M7824, only minor differences were observed in all immune cell populations after treatment with M7824mut (Fig. 2, Supplementary Figure 2). These results indicate that M7824 promotes activation of CD8+ T and NK cells in non-tumor-bearing mice.

M7824 has anti-tumor efficacy against breast and colon carcinomas

M7824 is able to effectively target both murine PD-L1 and TGFβ in the tumor microenvironment (Fig. 1B, F). We next investigated the therapeutic capacity of M7824 in multiple models of murine solid carcinomas. Administration of 20 mg/kg M7824, a clinically relevant dose,[29] significantly reduced growth of EMT6 breast carcinoma tumors as compared to treatment with PBS or M7824mut (Fig. 3A). Seventeen percent of mice treated with M7824 underwent complete tumor rejection (Fig. 3A, right

panel), which led to significant increases in median overall survival (OS) relative to mice treated with either PBS or M7824mut (Fig. 3B). No M7824mut-treated mice underwent complete tumor rejection (Fig. 3A). However, there was a trend of reduced tumor growth in M7824mut-treated mice with 29.4% of tumors being smaller than 500 mm^3 at day 27 versus 11.7% in PBS-treated animals (Fig. 3A). This translated to a significant increase in OS relative to PBS treatment (Fig. 3B). EMT6 tumor rechallenge of M7824-cured mice did not produce palpable tumors (Fig. 3C, D), indicating M7824 promotes long-term memory protection against these tumors.

Similar results were seen in mice bearing murine MC38 colon carcinoma tumors. M7824 treatment significantly reduced tumor growth, cured 30% of tumor-bearing mice (Fig. 3E), and increased median OS versus PBS treatment (Fig. 3F). Unlike in the EMT6 breast carcinoma model, M7824mut also promoted a significant reduction in MC38 tumor growth compared to PBS treatment but to a lesser extent than M7824 (Fig. 3E). M7824mut treatment
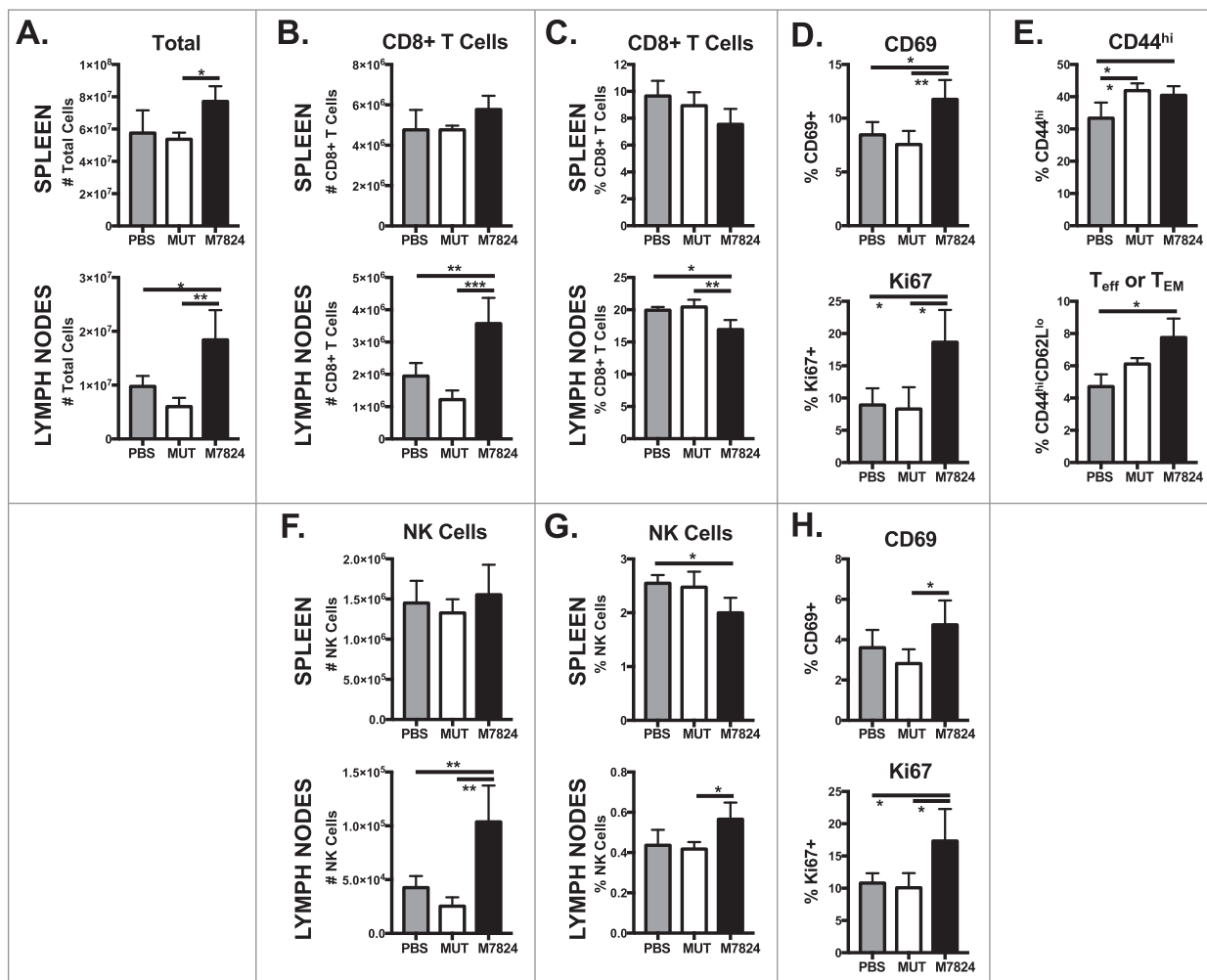
Figure 2. M7824 increases CD8+ and NK cell numbers in the lymph nodes and promotes their activation in non-tumor-bearing mice. Naïve Balb/c mice received MUT or M7824 i.p. on days 0, 2, and 4. Immune populations in the spleen and lymph nodes were analyzed by flow cytometry 3 or 7 days after the final treatment. Graphs show number of total cells (A), CD8+ T cells (B), and NK cells (F) or frequency (of total live cells) of CD8+ T cells (C), and NK cells (G) 3 days after last treatment. Phenotype of CD8+ T cells (D) and NK cells (H) was determined in the spleen 3 days after the last treatment. Maturation (CD44/CD62 L expression) of CD8+ T cells (E) was determined in the spleen 7 days after the last treatment. All graphs show mean ± SD. Data combined from 2 independent experiments, n = 3-5 mice per experiment.

did not induce tumor rejection (Fig. 3E) or a survival advantage versus PBS (Fig. 3F). Rechallenge of M7824-cured mice showed a memory response in two of three mice (Fig. 3G, H). While protection from rechallenge was not as robust as against EMT6 tumors (Fig. 3C, D), these results suggest that M7824 does support long-term protective memory generation against MC38 tumors.

We also examined the effect of M7824 on spontaneous metastasis. Using the murine 4T1 triple negative breast carcinoma (TNBC) model, we observed that M7824 treatment was able to limit primary tumor growth relative to PBS-treated mice (Supplementary Figure 3A) and reduced 4T1 metastasis to the lung (Supplementary Figure 3B, C). Together, these studies show that dual targeting of TGFβ and PD-L1 with M7824 promotes significant anti-tumor efficacy in multiple murine breast and colon carcinoma models.

CD8+ T and NK cells are responsible for the anti-tumor effects of M7824

Given that M7824 treatment activated both CD8+ T and NK cell populations in non-tumor-bearing mice (Fig. 2), we

hypothesized that CD8+ T cells and NK cells promote the anti-tumor efficacy of M7824. To test this, we depleted CD8+ T cells and NK cells in EMT6 tumor-bearing mice treated with M7824. The depletion efficiency for CD8+ T cells (Fig. 4A) and NK cells (Fig. 4B) was approximately 99% and 75–90% during the course of the experiment, respectively. As seen in Fig. 3, treatment of EMT6 tumor-bearing mice with M7824 promoted significant reduction in tumor burden and increased median OS. Depletion of CD8+ T cells (Fig. 4C, F) and NK cells (Fig. 4D, F) completely abrogated the therapeutic capacity of M7824. NK cell depletion in M7824-treated mice led to tumor growth (Fig. 4D, F) and median OS (Fig. 4G) similar to that seen in PBS-treated animals. In contrast, depletion of CD8+ T cells significantly exacerbated tumor growth (Fig. 4C, F) and decreased survival by a week (Fig. 4G) as compared to PBS-treated mice. Tumor burden and survival of mice depleted of both CD8+ T cells and NK cells mimicked the results seen with CD8+ T cell depletion (Fig. 4E-G). These results suggest that CD8+ T cells are required for basal therapeutic efficacy of M7824 against EMT6 tumors and can partially compensate for the loss of NK cells but not vice versa. In all, these studies show
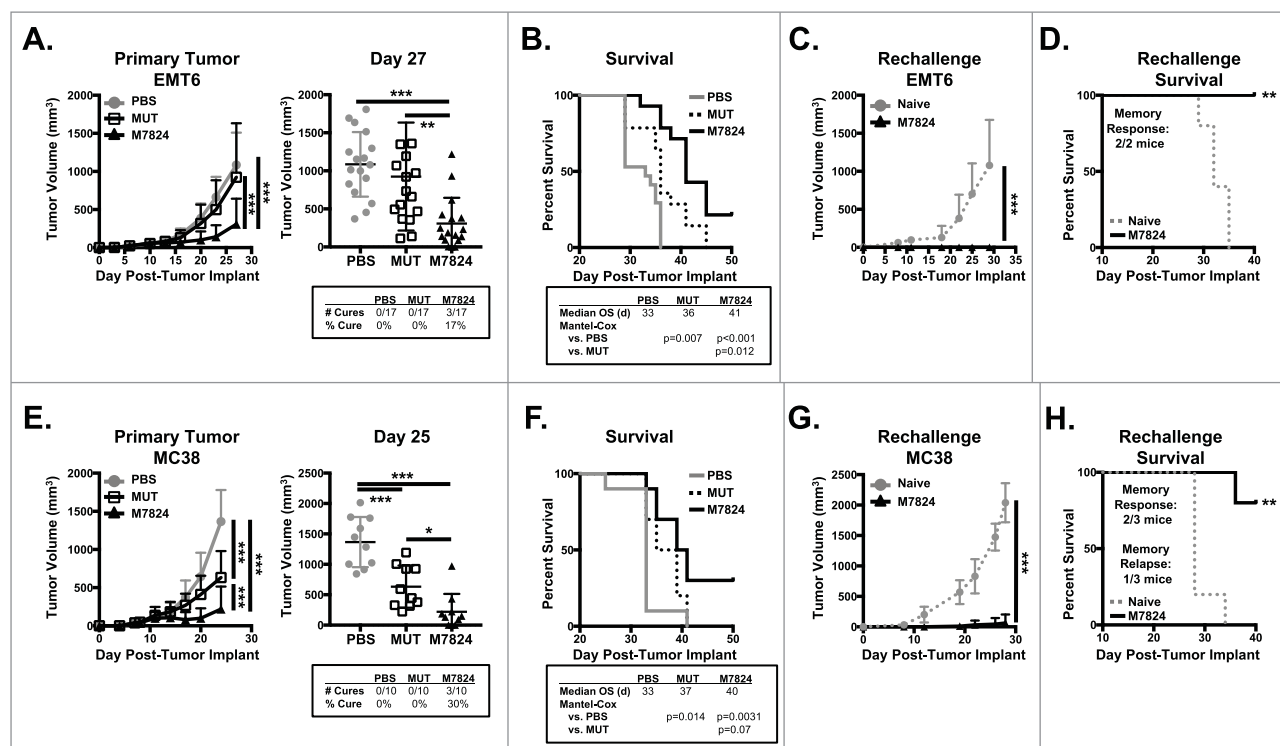
Figure 3. M7824 has anti-tumor efficacy against murine EMT6 breast and MC38 colon tumors. (A, B) EMT6 tumor cells were implanted as in Figure 1 and mice were treated at days 9, 11, and 13. Tumor volumes were measured and survival was tracked. (A) Primary tumor growth curves (left panel) and tumor volumes of individual animals (right panel, inset: number of cured mice) show mean ± SD. (B) Survival curves (inset: median overall survival (OS) in days) show % survival. (C, D) At least 1 month after tumor cure (day 94), cured mice and 5 naïve Balb/c were implanted with EMT6 tumor cells. (C) Tumor growth curves show mean ± SD. (D) Survival curves (inset shows # of mice with memory response) show % survival. Data are representative of 3 independent experiments, n = 10-20 mice. (E, F) 5 × 10⁵ MC38 tumor cells were implanted into female C57BL/6 mice and treated at days 9, 11, and 13. (E) Primary tumor growth curves (left panel) and tumor volumes of individual animals (right panel, inset: number of cured mice) show mean ± SD. (F) Survival curves (inset: median OS in days) show % survival. (G, H) At least 1 month after tumor cure (day 72), cured mice and 5 naïve C57BL/6 were implanted with MC38 tumor cells. (G) Tumor growth curves show mean ± SD. (H) Survival curves (inset: # of mice with memory response or relapse) show % survival. Data are representative of 2 independent experiments, n = 10 mice.

that both CD8+ T cells and NK cells are required for the anti-tumor efficacy of M7824.

We also performed CD4 depletion on EMT6 tumor-bearing mice to determine whether CD4+ T cells contributed to the anti-tumor efficacy of M7824. Ninety-nine percent reduction of CD4+ T cells (Supplementary Figure 4A) led to tumor rejection in 100% of the M7824-treated mice (Supplementary Figure 4B-D). Further interrogation of this phenomenon revealed that EMT6 tumors, even in the absence of M7824 treatment, are highly susceptible to CD4 depletion, as 90% of PBS-treated mice underwent complete tumor rejection when CD4+ T cells were depleted (Supplementary Figure 4E-G). Similar observations have been reported in other tumor models.[30]

M7824 induces a more active CD8+ and NK phenotype in EMT6 tumors

As CD8+ T cells and NK cells were required for anti-tumor effects of M7824, we examined these cell types in the tumor and spleen of EMT6 tumor-bearing mice after treatment with M7824. There were no changes to frequency or number of CD8+ T cells in the tumor or spleen upon M7824 treatment (Supplementary Figure 5A). However, there was a greater frequency of Ki67+ CD44hi CD8+ T cells in the tumor, indicating a greater proliferative capacity of these cells (Fig. 5A). In addition, there was a trend toward a larger population of CD44hi CD8+ T cells that also

expressed NKG2D in the TME (Fig. 5B), suggesting the accumulation of an activated, innate-like CD8+ T cell[31,32] in the TME. These phenotypic effects were exclusive to M7824-treated tumors, as M7824mut did not induce these changes (Fig. 5A, B). In contrast to the tumor, there was a significant increase in the frequency of effector (T_eff) or effector memory (T_EM) CD8+ T cell populations in the spleens of M7824-treated mice (Fig. 5C). Frequency of central memory (T_CM) CD8+ T cells was not increased with M7824 treatment (Fig. 5C). While we observed similar increases to the Ki67+ CD44hi CD8+ T cell population in the spleen as in the tumor, there was no increase in the frequency of NKG2D+ cells in M7824-treated mice (Fig. 5A, B).

In order to examine the function of CD8+ T cells upon M7824 treatment, we restimulated isolated CD44hi CD8+ T cells from the spleen with PMA and ionomycin. While the total frequency of IFNγ+ CD8+ T cells did not increase with treatment (Fig. 5D, upper panel), M7824-treated CD8+ T cells produced more IFNγ on a per cell basis (Fig. 5D, lower panel). In addition, a smaller frequency of CD8+ T cells from M7824-treated mice produced tumor necrosis factor alpha (TNFα) (Fig. 5E). This led to the overall frequency of IFNγ-single-producing CD8+ T cells to increase and TNFα-single-producing CD8+ T cells to decrease while having no effect on the IFNγ/TNFα double-producers (Fig. 5F). M7824mut treatment did not alter cytokine production of CD8+ T cells upon restimulation (Fig. 5D-F). These data suggest that M7824 treatment does
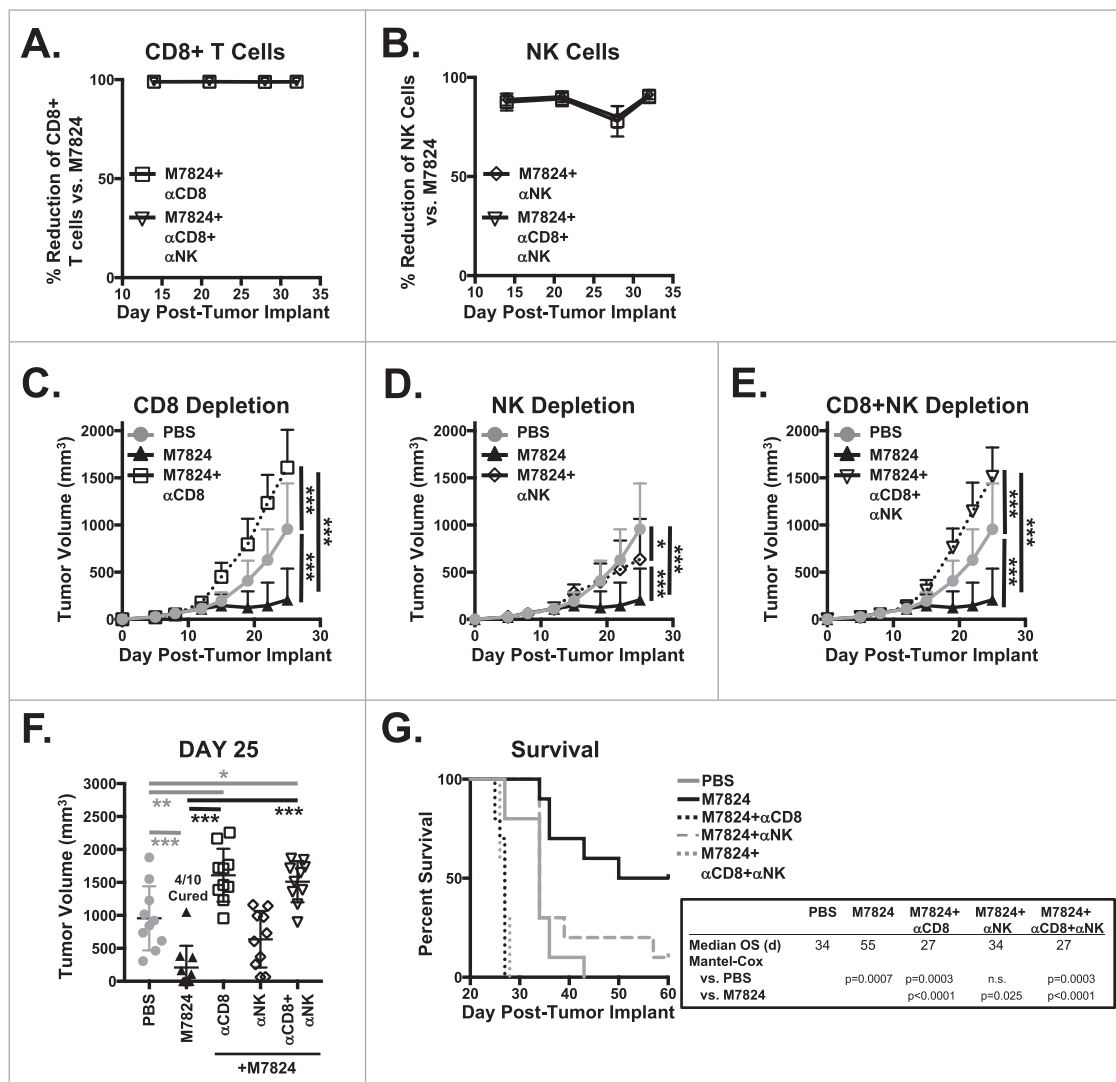
Figure 4. CD8+ T cells and NK cells are responsible for the anti-tumor efficacy of M7824. EMT6 tumor-bearing mice were treated as in Figure 1 with PBS or M7824. M7824-treated mice also underwent depletion of CD8, NK, or CD8 and NK cells. (A, B) Depletion efficiency was determined in the blood weekly by flow cytometry. Graphs show % reduction of CD8+ T cells (A) or NK cells (B) versus M7824-treated mice (set to 0%) as mean ± SD. (C, D, E) Primary tumor growth curves of mice that underwent CD8 (C), NK (D), or CD8 and NK (E) depletion show mean ± SD. (F) Graphs of tumor volumes of individual mice show mean ± SD. (G) Survival curves (inset: median OS in days) show % survival. Data represent 1 independent experiment, n = 10 mice.

increase the activity of CD8+ T cells, specifically skewing the population to produce IFNγ.

The effect of M7824 on NK cell phenotype was similar to that seen on CD8+ T cells. While there were no major changes in frequency or number of NK cells in the tumor or spleen (Supplementary Figure 5B), tumor-infiltrating NK cells displayed a more active, cytotoxic phenotype. M7824 treatment expanded the population of the most cytotoxic NK cell subset (CD27^{hi}CD11b^{hi}) (Fig. 5G). The frequency of Ki67+ NK cells also increased upon M7824 treatment (Fig. 5H). These effects were not observed in M7824mut-treated tumors or in the spleens of M7824-treated mice (Fig. 5G-I).

We did not observe significant changes to frequency or number of total CD4+ T cells (Supplementary Figure 6A), T$_{reg}$ (Supplementary Figure 6B), or myeloid-derived suppressor cell (MDSC) populations (Supplementary Figure 6C-E) in the tumor with M7824 treatment. Together, these results suggest that M7824 treatment elicits its anti-tumor activity by increasing activation of CD8+ T cells and NK cells.

M7824 treatment induces phenotypic changes to non-immune tumor-associated cells in the TME

EMT6 tumor cells produce high levels of TGFβ.[33] Given TGFβ's ability to work as both an autocrine and paracrine factor,[34] sequestration of TGFβ in the TME by M7824 (Fig. 1), as well as cytokine production by tumor-infiltrating lymphocytes (TILs) (Fig. 5), could lead to phenotypic changes to non-immune cells in the TME, such as tumor and stromal cells. No changes to non-immune CD45 negative cells were observed within 1 week following M7824 treatment (data not shown). However, 1 week after the final M7824 treatment (day 21), we observed a 3-fold increase in the expression of PD-L1 and MHC class II in the TME CD45 negative population (Supplementary Figure 7A, B). No changes were observed in MHC
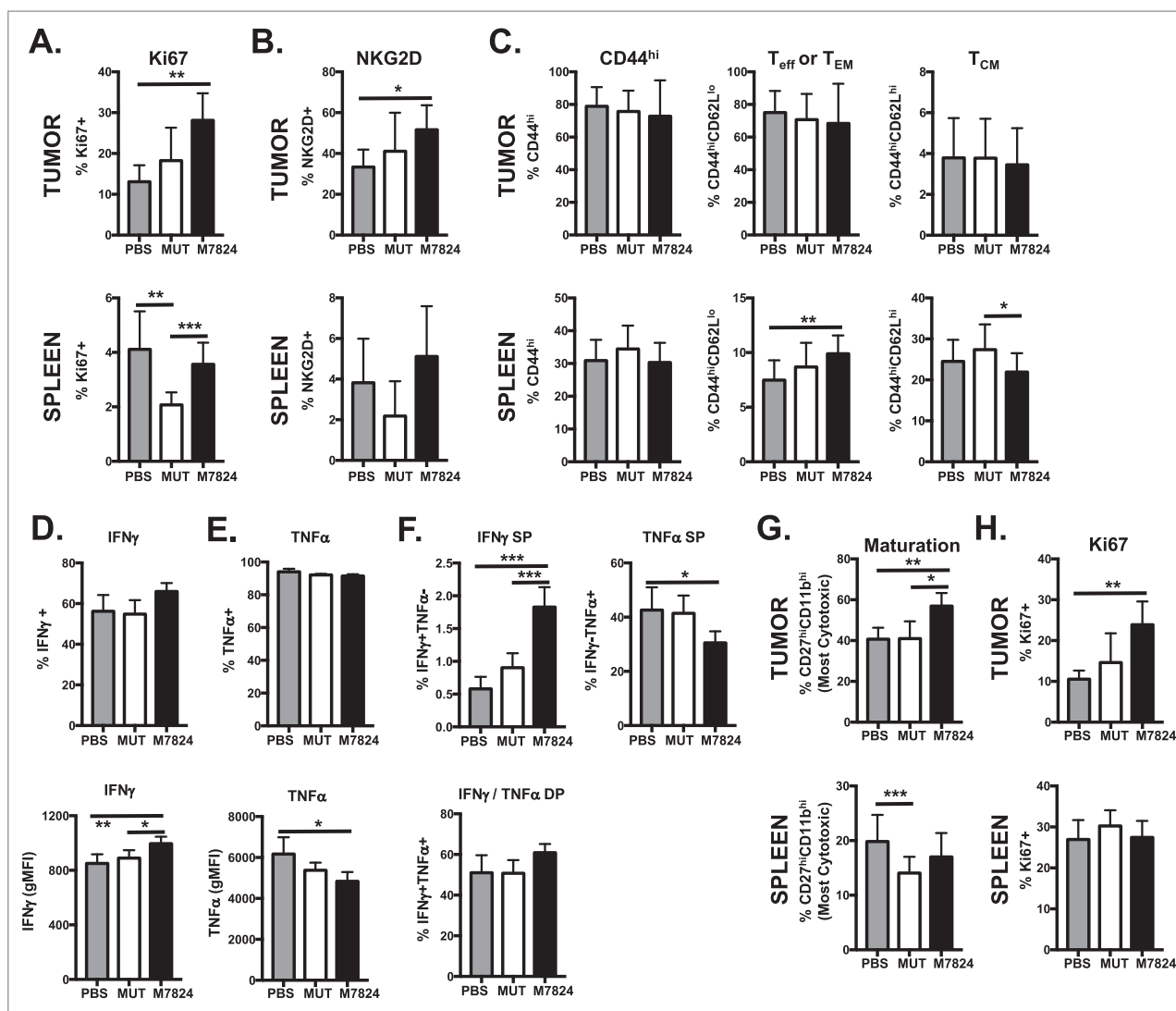
Figure 5. M7824 induces a more active CD8+ T and NK cell phenotype in the TME. EMT6 tumor-bearing mice were treated as in Figure 1. (A, B, C, G, H) Immune subsets in the tumor (top panels) or spleen (bottom panels) were examined 15 days after tumor implant by flow cytometry. CD8+ T cell expression of Ki67 (A), NKG2D (B), and maturation (CD44/CD62L) (C) were examined as well as NK cell maturation (CD27/CD11b) (G) and expression of Ki67 (H). Data combined from 2–3 independent experiments, n = 3-10 mice. (D, E, F) Isolated splenic CD8+ T cells were restimulated *ex vivo* with PMA and ionomycin for 4 hours. Expression of IFNγ (D, F) and TNFα (E, F) was determined by flow cytometry. Frequency of IFNγ single-producers (SP), TNFα SP, or IFNγ/TNFα double-producers (DP) in (F). Data are representative of 2 independent experiments, n = 5 mice. All graphs show mean ± SD.

class I expression as almost 100% of these cells expressed MHC class I in PBS-treated mice (Supplementary Figure 7C, D). Thus M7824 treatment does have an effect on tumor cell phenotype in the TME.

M7824 complete responders display a distinct immune compartment as compared to non-cured mice

Seventeen to 40% of M7824-treated mice underwent complete EMT6 tumor rejection (Figs. 3,4), and this effect was apparent in the immune compartment 35 days after tumor implant. M7824-cured mice displayed a splenic immune compartment typical of mice that have undergone immune resolution. The total number of splenocytes (Supplementary Figure 8A), CD8+ T cells (Supplementary Figure 8B), and NK cells (Supplementary Figure 8D) were significantly decreased in M7824-complete responders. However, the frequencies of CD8+ T cells (Supplementary Figure 8B) and NK cells (Supplementary

Figure 8D) were approximately double as compared to those in PBS- and M7824-tumor-bearing mice. In the CD8+ T cell compartment in complete responders compared to tumor-bearing mice, the frequency of naïve CD8+ T cells was significantly decreased by 30%, corresponding with an equally greater frequency of CD8+ T cells with an T_{eff} or T_{EM} phenotype (Supplementary Figure 8C). There were no differences in T_{CM} CD8+ T cell frequencies (Supplementary Figure 8C). In the NK cell compartment in cured mice, the frequency of the most cytotoxic NK cell population was decreased by 50%, while the most mature NK population increased as compared to tumor-bearing animals (Supplementary Figure 8E). NK cells from cured mice maintained a significant increase in the frequency of activated NKp46+ cells (Supplementary Figure 8F) as seen at earlier time points (Fig. 5). The differences observed between the CD8+ T and NK cells in cured versus non-cured mice suggest that a greater CD8+ T cell or NK cell response may be responsible for the ability to completely reject tumors.

M7824 combination with Ad-TWIST vaccine improves anti-tumor response versus M7824 monotherapy

While tumor growth decreased and OS improved with M7824 treatment, only 17–40% of mice underwent complete tumor rejection (Figs. 3, 4). Since M7824 treatment enhanced the activation of CD8+ T cells, we hypothesized that combination therapy with a vaccine targeting a tumor-associated antigen (TAA) would improve anti-tumor efficacy. Thus, we combined M7824 with an adenovirus vaccine encoding the murine tumor-associated antigen TWIST1 (Ad-TWIST), which is expressed by EMT6 tumors (Supplementary Figure 9). TWIST1 is involved in EMT, metastasis, and angiogenesis,[35,36] and previous studies have shown that vaccination against TWIST1 decreases murine tumor growth and spontaneous metastasis.[37,38] EMT6 tumor-bearing mice were administered M7824 followed by three doses of Ad-TWIST weekly. While vaccination alone did not affect tumor growth or median OS as compared with PBS treatment, the combination of M7824 with Ad-TWIST significantly reduced the tumor burden (Fig. 6A) and increased median OS by 40% (Fig. 6B). While the decrease in tumor burden was similar between M7824 monotherapy and M7824/Ad-TWIST combination therapy (Fig. 6A), the combination of M7824 and Ad-TWIST did increase median OS by 31% compared to M7824 monotherapy (Fig. 6B). Both M7824 monotherapy and M7824/Ad-TWIST combination therapy induced the generation of protective memory, as all cured mice remained tumor-free after rechallenge (Fig. 6C, D). These results support the use of M7824 with cancer vaccines to improve anti-tumor efficacy.

Dual targeting of TGFβ and PD-L1 is required for synergistic activity of M7824 in combination with Ad-TWIST vaccine

The αPD-L1 moiety of M7824 is based on avelumab. Treatment of EMT6 tumor-bearing mice with αPD-L1/avelumab led to a reduction in tumor burden (Fig. 6E) and increases in median OS (Fig. 6F) similar to that observed with M7824 monotherapy. M7824 promoted a robust generation of protective memory, as 3/3 M7824-cured mice were protected against EMT6 tumor rechallenge (Fig. 6G, H). Only 1/2 αPD-L1-cured mice were protected from tumor rechallenge (Fig. 6G, H). The anti-tumor efficacy of both αPD-L1 and M7824 outperformed M7824mut (Fig. 6E, F).

When αPD-L1 was given in combination with Ad-TWIST vaccine, however, the anti-tumor efficacy of αPD-L1 therapy was lost. αPD-L1/Ad-TWIST combination-treated mice had tumor burden (Fig. 6I) and median OS (Fig. 6J) similar to that found in PBS- and M7824mut-treated animals. This is in distinct contrast to the increased OS observed in M7824/Ad-TWIST combination-treated mice versus PBS- and M7824mut-treated mice (Fig. 6J). Additionally, the combination of M7824mut with vaccine did not increase anti-tumor efficacy relative to PBS treatment (Fig. 6I, J). These results demonstrate that M7824, but not αPD-L1, is amenable to combination with cancer vaccines. Importantly, these results demonstrate that both blockade of PD-L1 and TGFβ sequestration are required for synergistic anti-tumor efficacy in combination with a cancer vaccine.

Discussion

Activating the immune system for therapeutic benefit against cancer has recently become a reality with the use of immune checkpoint-targeted mAbs, such as αPD-L1/αPD-1 antibodies. However, many patients see no clinical benefit with αPD-L1/αPD-1 therapy, even if their tumors express the targeted ligand.[1] One explanation for this is the presence of other molecules in the tumor microenvironment, such as the immunosuppressive cytokine TGFβ. In these studies, we show that dual inhibition of PD-L1- and TGFβ-mediated suppressive pathways by the novel agent M7824 produced substantial anti-tumor efficacy against murine models of breast and colon carcinoma. M7824 decreased tumor burden and increased OS versus control-treated mice. Importantly, both the ability to block PD-L1 and sequester TGFβ was required for the efficacy of M7824, as TGFβ sequestration alone by M7824mut did not improve tumor responses. This is in contrast to other studies showing that blocking TGFβ1 and TGFβ2 alone was sufficient to improve anti-tumor efficacy in murine tumor models.[39] However, those studies began treatment on the day of tumor implant, which may improve immune cell priming before tumor establishment and lead to altered development of an immunosuppressive microenvironment.

Blocking PD-L1 played a major role in M7824-mediated therapy, as treatment with the parent molecule avelumab (αPD-L1), which only blocks PD-L1, showed similar anti-tumor efficacy. However, M7824 combination with Ad-TWIST vaccine further improved OS versus M7824 monotherapy, similar to results in studies using a TGFβ blocking antibody in combination with an αPD-1 antibody and vaccine.[39] This synergistic effect was not observed with αPD-L1 and vaccine combination therapy. In fact, the combination of αPD-L1 and vaccine completely abrogated the anti-tumor efficacy of αPD-L1. How M7824 is able to synergize with a therapeutic cancer vaccine while αPD-L1 therapy does not is currently under investigation. Preliminary data suggest that the distribution of CD8+ T cells to the spleen and lymph nodes may be decreased on αPD-L1 but not M7824 treatment (data not shown). This may prevent proper CD8+ T cell priming upon vaccination after αPD-L1 treatment. Alternatively, the presence of TGFβ in both the periphery as well as the tumor of αPD-L1-treated animals may prevent CD8+ T cell activation upon vaccination, which M7824 can overcome as it both sequesters plasma TGFβ1 and prevents TGFβ-induced signaling. TGFβ is also known to regulate the development and function of T_{reg},[28] which play an important role in CD8+ T cell activation and function. Thus, it is possible that M7824 may decrease T_{reg} function during CD8+ T cell activation and priming after vaccination. Previous studies have shown that M7824 treatment of human T_{reg} decreases their suppressive function.[40] Collectively, the results presented here suggest that the use of the novel bifunctional agent M7824 does have potential advantages versus pre-existing αPD-L1/αPD-1 therapies and should be further investigated for use in the clinic, including in combination with therapeutic cancer vaccines as well as other immunotherapies.

M7824 combines the ability to block PD-L1 and sequester TGFβ into a single agent. Whether M7824, as a single bifunctional
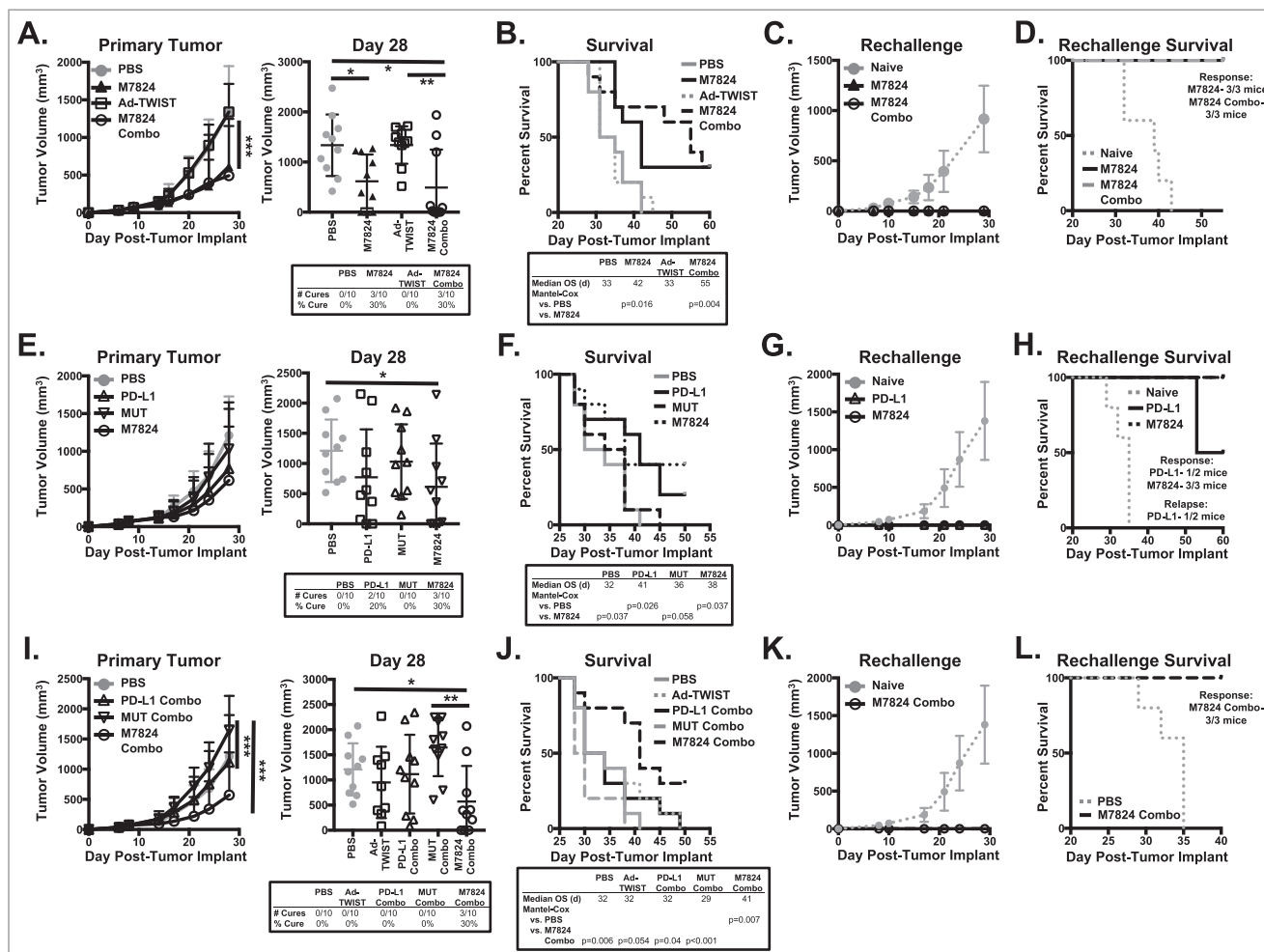
Figure 6. M7824 combination with Ad-TWIST improves anti-tumor efficacy versus M7824 or Ad-TWIST monotherapy. (A, B, E, F, I, J) EMT6 tumor-bearing mice were treated with PD-L1, MUT, or M7824 at days 10, 12, and 14 followed by vaccination with Ad-TWIST at days 16, 23, and 30. (A, E, I) Primary tumor growth curves (left panel) and tumor volumes of individual animals (right panel, inset: # of cured mice) show mean±SD. (B, F, J) Survival curves (inset: median OS in days) show % survival. (C, D, G, H, K, L) Cured mice from A, E, I, and 5 naïve Balb/c mice were implanted with EMT6 tumor cells at least 1 month after tumor rejection. (C, G, K) Tumor growth curves show mean±SD. (D, H, L) Survival curves (inset: # of mice with memory response or tumor relapse) show % survival. Data is representative of 2–3 independent experiments, n = 10 mice.

molecule, elicits better anti-tumor responses than the use of αPD-L1 in combination with a TGFβ inhibitor or TGFβ-targeted mAb remains to be explored. However, we hypothesize that M7824 will have increased anti-tumor efficacy since we have shown that it accumulates in the tumor by binding to PD-L1. By increasing the concentration of M7824 at the tumor site, it allows for local sequestration of TGFβ, which is produced in high levels by both tumor and tumor-associated immune cells.[13,41] Importantly, our results show that even though M7824 significantly decreases plasma TGFβ1 levels, it still has the ability to suppress TGFβ-dependent signaling in the TME. This was dependent on accumulation of M7824 in the tumor, as M7824mut decreased TGFβ1 levels in the plasma but did not bind to TME-expressed PD-L1 and did not decrease TGFβ-dependent signaling in the TME. Why M7824 treatment decreased TGFβ-dependent activation of SMAD2 but not SMAD3 remains to be determined. However, it is known that SMAD2 and SMAD3 have different thresholds and kinetics of activation upon TGFβ stimulation.[42-44] Thus, it possible that SMAD3 is also affected by M7824, as has been seen in human tumor cell lines.[45] Targeting TGFβ sequestration to the tumor site may also reduce the potential adverse effects of using a

systemic TGFβ inhibitor, such as cardiac toxicity, development of neoplasms, and re-activation of dormant cancer cells seen in pre-clinical models with some TGFβR-targeted small molecule inhibitors.[23]

TGFβ is a known suppressor of tumor progression early in tumor development.[13,14] Some studies have shown that lower TGFβ serum level correlates with worse prognosis,[46] and loss of TGFβ signaling accelerates tumor growth. In our studies, sequestration of TGFβ did not promote tumor growth.[20,22,47] In fact, M7824 displayed potent anti-tumor activity in multiple murine tumor models. This could be due to the treatment schedule of M7824, which was administered after the tumors were well-established. In addition, the administration of M7824 to EMT6, MC38, or 4T1 tumor cells in vitro induced no changes to tumor cell proliferation over the course of 5 days (data not shown).

In our studies, the anti-tumor effects of M7824 were highly dependent on CD8+ T cell and NK cells. Loss of these cell populations by antibody-mediated depletion abrogated the therapeutic capacity of M7824. Immunophenotypic analysis supported this finding, as M7824 promoted an activated CD8+

T and NK cell phenotype in both tumor- and non-tumor-bearing mice. This is in agreement with the effects of blocking PD-L1/PD-1 and TGFβ immunosuppressive pathways during T and NK cell responses.[48-50] Although the PD-L1/PD-1 interaction and TGFβ are known to regulate T and NK cell exhaustion and anergy,[48,51,52] no decreases were observed in the expression of phenotypic markers associated with exhaustion, such as PD-1, Tim-3, or VISTA (data not shown). As functional immune exhaustion is dependent on a balance of activation and inhibitory/exhaustive signals,[53] it is possible that the immune-activating capabilities of M7824 are able to overcome any existing expression of these receptors. Alternatively, since these "exhaustion"-related receptors are normally expressed upon immune cell activation to prevent excessive immune responses,[53] a distinct reduction in their expression may not be observed due to the immune-activating nature of M7824.

The expression of TGFβ receptor on naïve CD8+ T cells maintains a stimulation threshold restricting T cell activation. Genetic loss of TGFβ receptor or suppression of TGFβ signaling decreases this threshold and allows for activation of CD8+ T cells against lower affinity antigens,[54] such as TAAs. Thus, sequestration of TGFβ by M7824 may increase the diversity of responding CD8+ T cell clones during anti-tumor immune responses. This is important, as a more diverse T cell repertoire promotes successful and long-lasting anti-tumor immunity.[55-57] Studies investigating T cell repertoire diversity during M7824 treatment may also provide insight into rational immunotherapy combination design. For example, we observed improved anti-tumor responses when M7824 was given in combination with a cancer vaccine. Vaccination against TAAs in cancer patients is known to induce greater tumor antigen-specific immune responses and can also lead to responses against other TAAs not encoded by the vaccine.[58,59] By lowering the T cell activation threshold with TGFβ sequestration and supporting expanded T cell activation and function by blocking PD-L1, M7824 may further improve these antigen-specific responses and lead to better clinical outcome.

In conclusion, the studies presented here demonstrate that dual targeting of PD-1/PD-L1 and TGFβ immunosuppressive pathways with the novel bifunctional agent M7824 promotes potent anti-tumor responses in murine models of human solid carcinomas. Furthermore, these results support clinical development of M7824 as both a monotherapy and in combination with other immunotherapies, such as therapeutic cancer vaccines. A phase I clinical study of M7824 in heavily pretreated patients with advanced solid carcinomas is ongoing (NCT02517298).[29] M7824 was shown to be well-tolerated, with adverse events similar to those seen with other αPD-L1/PD-1 mAbs. In addition, there was evidence of clinical efficacy seen across all dose levels (0.3-20 mg/kg). This included one ongoing confirmed complete response in a cervical cancer patient (10 mg/kg), one durable partial response in a patient with pancreatic cancer (3 mg/kg), and two cases of prolonged stable disease in pancreatic (3 mg/kg) and carcinoid (1 mg/kg) cancer patients.[29] Phase II studies utilizing M7824, including a study combining M7824 and a therapeutic cancer vaccine targeting prostate specific antigen (PSA) or carcinoembryonic antigen (CEA) plus mucin 1 (MUC1), are currently planned or ongoing in multiple tumor types.

Materials and methods

Tumor cell lines

Murine breast carcinoma cells EMT6 and 4T1 were obtained from American Type Culture Collection (ATCC) and 4T1-pSMAD2-luc was kindly provided by EMD Serono. All cell lines were cultured according to the manufacturer's instructions. Murine colon carcinoma MC38 cells are as described.[60] All cell lines were free of *mycoplasma* as determined by MycoAlert Mycoplasma Detection Kit (Lonza) and were used at low passage numbers.

Reagents

The following biological agents were generously provided by EMD Serono under a Cooperative Research and Development Agreement with NCI: avelumab (designated as αPD-L1), a fully human αPD-L1 (IgG1); M7824, a fully human bifunctional molecule comprised of the extracellular domain of human TGFβRII (TGFβ Trap) linked to the C-terminus of αPD-L1 heavy chain; and M7824mut, a fully human molecule comprised of human TGFβRII bound to a mutated αPD-L1 moiety. Recombinant murine TGFβ1 was from R&D Systems and recombinant murine IFNγ was obtained from PeproTech. CD8 (2.43) and CD4 (GK1.5) depletion antibodies were obtained from BioXcell and the NK (anti-asialo-GM1) depletion antibody was from Wako Chemicals. Adenovirus encoding the murine TWIST1 gene (Ad-CMV-TWIST, referred to as Ad-TWIST) was from Vector Biolabs.

Flow cytometry and antibodies

Preparation of cells for flow cytometry was performed using the BD Cytofix/Cytoperm Kit (BD Biosciences) according to the manufacturer's instructions. Anti-H-2D^d (34-2-12), -H-2K^d (SF1-1.1), -I^A/I^E (M5/114), -GR1 (RB6-8C5), -FoxP3 (R16-715), -CD62L (MEL-14), -CD44 (IM7), -CD3Ɛ (2C11), -CD274 (MIH5), -CD19 (1D3), -CD11b (M1/70), -IFNγ (XMG1.2), -TNFα (MPG-XT22) were purchased from BD Biosciences. Anti-CD8α (53-6.7), -Ki67 (SolA15), -Eomes (Dan11Mag), -FoxP3 (FJK-16s), -CD69 (H1.2F3), -NKp46 (29A1.4), -NKG2D (CX5), -CD279 (J43) were from eBioscience. Anti-CD8β (53-5.8), -VISTA (MH5A), -Tim-3 (B8.2C12), -Ly6C (HK1.4), -Ly6G (1A8), -CD49b (DX5), -CD45.2 (104), -CD4 (RM4-5, RM4-4), -CD25 (PC61), -CD122 (TMβ1) were purchased from Biolegend. Anti-SMAD2/3 (D7G7) and anti–phospho-SMAD2/3 (D27F4) were from Cell Signaling Technology, and anti-TGFβRII was from R&D Systems. Anti-human (H+L) secondary antibody and Live/Dead Fixable Dead Cell Stain were from Invitrogen. Matched isotypes were obtained from the aforementioned manufacturers. Flow cytometry ($\geq 1 \times 10^5$ events acquired per sample) was performed on a BD FACS-Verse or LSRII Fortessa flow cytometer (Beckton Dickinson) and analyzed with FlowJo FACS Analysis Software (Treestar). Cell populations were identified as follows: CD8+ T cells: live/CD45.2+/CD3+/CD8+; CD4+ T cells: live/CD45.2+/CD3+/CD4+/FoxP3 negative; CD4+ T$_{reg}$: live/CD45.2+/CD3+/CD4+/FoxP3+; NK cells: live/CD45.2+/CD3-/CD49b+; Gr1+ cells: live/CD45.2+/CD11b+/Gr1+; Granylocytic MDSC/Neutrophils: live/CD45.2+/CD11b+/Ly6Ghi/Ly6Clo; Monocytic MDSC/Monocytes: live/CD45.2+/CD11b+/Ly6Glo/Ly6Chi;

non-immune, tumor cell compartment: live/CD45 negative. All frequencies of cells expressing phenotypic proteins were generated by subtracting the frequency of respective isotype, typically set between 1–5%.

Mice

Six- to 10-week old female Balb/c and C57BL/6 mice were obtained from the National Cancer Institute's Frederick Cancer Research Facility, Frederick, MD, and were maintained in microisolator cages under specific pathogen-free conditions in accordance with the Association for Assessment and Accreditation of Laboratory Animal Care (AAALAC) guidelines. All experimental studies were carried out under approval of the NIH Intramural Animal Care and Use Committee.

Murine tumor studies

For murine breast carcinoma studies, 2.5×10^5 EMT6 tumor cells or 5×10^4 4T1 tumor cells were orthotopically implanted subcutaneously (s.c.) into the mammary fat pad of female Balb/c mice. For murine colon carcinoma studies, 5×10^5 MC38 tumor cells were implanted s.c. into the right flank of female C57BL/6 mice. Mice were randomized based on tumor size and treatments were initiated when tumors reached 50–100mm[3]. Mice received three doses of $400\mu g$ αPD-L1, $492\mu g$ M7824mut, or $492\mu g$ M7824 (all equivalent to 20 mg/kg) via intraperitoneal injection (i.p.) in all experiments. For vaccine combination studies, animals received 10^{10} Ad-TWIST virus particles (VP) s.c. beginning 7 days after the initiation of treatment with αPD-L1, M7824mut, or M7824 and then weekly for a total of three doses. All tumors were measured twice weekly using calipers and tumor volumes were determined using the formula (length^2 $\times$ width)/2. For tumor rechallenges, EMT6 or MC38 tumor cells were implanted at the numbers and locations listed above into cured mice (and naïve controls) at least 1 month after tumor rejection.

4T1 lung metastasis

For quantitative analysis of 4T1 lung metastasis in tumor-bearing mice, lungs were processed and plated as previously described, based on 4T1 exclusive resistance to 6-thioguanine (6-TG).[37,61] Briefly, lung single-cell suspensions were obtained through enzymatic digestion and plated in 6-TG containing medium at 37 °C/ 5%CO$_2$. After 10–14 days in culture, cell colonies resulting from 4T1 single-cell clonal expansion were fixed with methanol, washed, stained with methylene blue, and enumerated.

Depletion studies

$100\mu g$ anti-CD4 (GK1.5) or anti-CD8 (2.43) depletion antibodies were administered i.p. to tumor-bearing mice on days 5, 6, and 7 post-tumor implant and then once weekly for the duration of the experiment. $25\mu l$ anti-NK (anti-asialo-GM1) depletion antibody was administered in a total of $100\mu l$ PBS i.p. on days 5 and 7 post-tumor implant followed by every 3 days until day 18 and then every 5 days through the duration of the experiment. Anti-CD8 and anti-NK antibodies were given in combination according to the aforementioned schedule. Blood was obtained weekly from three mice per group to determine immune cell population depletion efficiency by flow cytometry.

Flow cytometric analysis of immune and tumor cells

Spleens and lymph nodes (cervical, brachial, axillary and inguinal) were harvested, smashed using $120\mu M$ nylon sheets, filtered through a $70\mu M$ filter, and subjected to ACK lysis. Tumors were harvested, cut into 2 mm pieces and processed using the gentle-MACS Dissociator according to the manufacturer's instructions (Miltenyi Biotec). After digestion, single cell suspensions were filtered through a $70\mu M$ filter. TILs were enriched using a 44%/ 67% Percoll (GE Healthcare) gradient. All cell counts were performed using 123count eBeads (eBioscience). Approximately 1– 10×10^6 immune cells were stained for flow cytometry.

CD8+ T cell restimulation

CD8+ T cells were isolated by negative selection from spleens of EMT6-tumor bearing mice at day 15 post-tumor implant using the CD8α+ T Cell Isolation Kit (Miltenyi Biotec) according to the manufacturer's instructions. 1×10^6 CD8+ T cells were stimulated with nothing or 50 ng/ml PMA and 500 ng/ml ionomycin for 4 hours. Intracellular IFNγ and TNFα production were detected by flow cytometry.

Immunoblot analysis

Protein lysates from MC38, EMT6 or 4T1 tumor cell lines were prepared with Cell Lysis Buffer (Cell Signaling) supplemented with 1 mM phenylmethanesulfonyl fluoride (Sigma-Aldrich). Lysates from 5×10^5 cells were resolved by SDS-PAGE and transferred to PVDF membranes using standard techniques and blocked using 5% bovine serum albumin (BSA). Membranes were incubated overnight at 4 °C with either anti-TWIST (Twist2C1a) from Santa Cruz Biotechnology or β-actin from Cell Signaling. Membranes were then incubated with appropriate secondary antibodies conjugated with IRDye-680 and visualized using the Odyssey Infrared Imaging System (LI-COR Biosciences).

Quantitation of TGFβ isoforms in mouse plasma

Platelet-poor plasma was collected as previously described.[62,63] TGFβ isoforms were measured using TGFβ Premixed Magnetic Luminex Performance Assay kit (R&D Systems, Cat# FCSTM17) according to the manufacturer's instructions. Quantification and analysis were performed with the Bio-Plex MAGPIX reader and Bio-Plex Manager software (Bio-Rad). Detection of TGFβ isoforms was performed both with and without acid-activation to determine the total level of active TGFβ1/2/3 (without acid activation) and total TGFβ1/2/3 (with acid activation). The limit of detection for TGFβ1 was 35.187 pg/ml, TGFβ2 was 16.953 pg/ ml, and TGFβ3 was 55.574 pg/ml.

Measurement of SMAD activation in mouse tumor samples

EMT6 tumors were sectioned, weighed, and snap-frozen in liquid nitrogen prior to analysis of SMAD2/3/1/5 activation by capillary

Western blot. Analyses were performed using the reagents provided by the vendor as previously described.[64] Briefly, tumor lysates (approximately 40 ng protein) were mixed with 1x SDS master mix containing sample buffer, DTT and fluorescently labeled standards and were heated at 70 °C for 10 minutes before being loaded into Peggy Sue (ProteinSimple) for analysis. Chemiluminescence was captured and quantified. Digital images were analyzed by Compass software (ProteinSimple). Target protein quantities were determined based on peak areas. The antibodies used in the study were: anti-Smad1/5 pS463/465, anti-Smad5, anti-Smad2 & anti-Smad3 (Cell Signaling Technology); anti-Smad3 pS423/425 & anti-Smad1 (Abcam), anti-Smad2 pS465/467 (Millipore), loading control anti-Vinculin (Sigma Aldrich), and horseradish peroxidase (HRP) conjugated anti-rabbit or anti-mouse secondary antibodies (ProteinSimple or Jackson ImmunoResearch).

Luciferase assay

Detection of luciferase was performed using Bright-Glo Luciferase Assay System (Promega) according to the manufacturer's instructions. In experiments where cells were pre-treated with biologics prior to TGFβ addition, luciferase was quantified at 1 hour post TGFβ addition, corresponding to the approximate peak of SMAD2 phosphorylation (Supplemental Figure 1C). Alternatively, in experiments where cells were treated with biologics after TGFβ addition, luciferase was quantified at 6 hours after TGFβ addition to allow for significant degradation of luciferase protein ($t_{1/2} = 2$ hours) following cessation of TGFβ-induced SMAD2 phosphorylation.

Statistics

Statistical analyses were performed in GraphPad Prism 7 (GraphPad Software). Unless otherwise stated, one-way ANOVA with Tukey's multiple comparisons was used for statistical analysis for data presented in bar graphs or scatter plots. Two-way ordinary ANOVA was used to analyze tumor growth curves. Survival was analyzed using Log-rank (Mantel-Cox) test. Statistical significance was set at $p < 0.05$. $^*p < 0.05$, $^{**}p < 0.005$, $^{***}p < 0.001$.

Disclosure of potential conflicts of interest

No potential conflicts of interest were disclosed.

References

1. Postow MA, Callahan MK, Wolchok JD. Immune checkpoint blockade in cancer therapy. J Clin Oncol. 2015;33:1974–82. doi:10.1200/JCO.2014.59.4358. PMID:25605845
2. Zou W, Wolchok JD, Chen L. PD-L1 (B7-H1) and PD-1 pathway blockade for cancer therapy: Mechanisms, response biomarkers, and combinations. Sci Transl Med. 2016;8:328rv4. doi:10.1126/scitranslmed.aad7118.
3. Hamanishi J, Mandai M, Iwasaki M, Okazaki T, Tanaka Y, Yamaguchi K, Higuchi T, Yagi H, Takakura K, Minato N, et al. Programmed cell death 1 ligand 1 and tumor-infiltrating CD8+ T lymphocytes are prognostic factors of human ovarian cancer. Proc Natl Acad Sci U S A. 2007;104:3360–5. doi:10.1073/pnas.0611533104. PMID:17360651
4. Qing Y, Li Q, Ren T, Xia W, Peng Y, Liu GL, Luo H, Yang YX, Dai XY, Zhou SF, et al. Upregulation of PD-L1 and APE1 is associated with tumorigenesis and poor prognosis of gastric cancer. Drug Des Devel Ther. 2015;9:901–9. doi:10.2147/DDDT.S75152. PMID:25733810
5. Robert C, Schachter J, Long GV, Arance A, Grob JJ, Mortier L, Daud A, Carlino MS, McNeil C, Lotem M, et al. Pembrolizumab versus ipilimumab in advanced melanoma. N Engl J Med. 2015;372:2521–32. doi:10.1056/NEJMoa1503093. PMID:25891173
6. Topalian SL, Sznol M, McDermott DF, Kluger HM, Carvajal RD, Sharfman WH, Brahmer JR, Lawrence DP, Atkins MB, Powderly JD, et al. Survival, durable tumor remission, and long-term safety in patients with advanced melanoma receiving nivolumab. J Clin Oncol. 2014;32:1020–30. doi:10.1200/JCO.2013.53.0105. PMID:24590637
7. Borghaei H, Paz-Ares L, Horn L, Spigel DR, Steins M, Ready NE, Chow LQ, Vokes EE, Felip E, Holgado E, et al. Nivolumab versus docetaxel in advanced nonsquamous non-small-cell lung cancer. N Engl J Med. 2015;373:1627–39. doi:10.1056/NEJMoa1507643. PMID:26412456
8. Carbone DP, Reck M, Paz-Ares L, Creelan B, Horn L, Steins M, et al. First-line nivolumab in stage IV or recurrent non-small-cell lung cancer. N Engl J Med. 2017;376:2415–26. doi:10.1056/NEJMoa1613493. PMID:28636851
9. Apolo AB, Infante JR, Balmanoukian A, Patel MR, Wang D, Kelly K, Mega AE, Britten CD, Ravaud A, Mita AC, et al. Avelumab, an anti-programmed death-ligand 1 antibody, in patients with refractory metastatic urothelial carcinoma: results from a multicenter, phase Ib study. J Clin Oncol. 2017;35:2117–24. doi:10.1200/JCO.2016.71.6795. PMID:28375787
10. Bellmunt J, de Wit R, Vaughn DJ, Fradet Y, Lee JL, Fong L, Vogelzang NJ, Climent MA, Petrylak DP, Choueiri TK, et al. Pembrolizumab as second-line therapy for advanced urothelial carcinoma. N Engl J Med. 2017;376:1015–26. doi:10.1056/NEJMoa1613683. PMID:28212060
11. Kaufman HL, Russell J, Hamid O, Bhatia S, Terheyden P, D'Angelo SP, Shih KC, Lebbé C, Linette GP, Milella M, et al. Avelumab in patients with chemotherapy-refractory metastatic Merkel cell carcinoma: a multicentre, single-group, open-label, phase 2 trial. Lancet Oncol. 2016;17:1374–85. doi:10.1016/S1470-2045(16)30364-3. PMID:27592805
12. Nghiem PT, Bhatia S, Lipson EJ, Kudchadkar RR, Miller NJ, Annamalai L, Berry S, Chartash EK, Daud A, Fling SP, et al. PD-1 blockade with pembrolizumab in advanced Merkel-cell carcinoma. N Engl J Med. 2016;374:2542–52. doi:10.1056/NEJMoa1603702. PMID:27093365
13. Lebrun JJ. The dual role of TGFβ in human cancer: from tumor suppression to cancer metastasis. ISRN Mol Biol. 2012;2012:381428. doi:10.5402/2012/381428. PMID:27340590
14. Principe DR, Doll JA, Bauer J, Jung B, Munshi HG, Bartholin L, Pasche B, Lee C, Grippo PJ. TGF-beta: duality of function between tumor prevention and carcinogenesis. J Natl Cancer Inst. 2014;106: djt369. doi:10.1093/jnci/djt369. PMID:24511106
15. Travis MA, Sheppard D. TGF-beta activation and function in immunity. Annu Rev Immunol. 2014;32:51–82. doi:10.1146/annurev-immunol-032713-120257. PMID:24313777
16. Hossain DM, Panda AK, Manna A, Mohanty S, Bhattacharjee P, Bhattacharyya S, Saha T, Chakraborty S, Kar RK, Das T, et al. FoxP3 acts as a cotranscription factor with STAT3 in tumor-induced regulatory T cells. Immunity. 2013;39:1057–69. doi:10.1016/j.immuni.2013.11.005. PMID:24315995
17. Moo-Young TA, Larson JW, Belt BA, Tan MC, Hawkins WG, Eberlein TJ, Goedegebuure PS, Linehan DC. Tumor-derived TGF-beta

mediates conversion of CD4+Foxp3+ regulatory T cells in a murine model of pancreas cancer. J Immunother. 2009;32:12–21. doi:10.1097/CJI.0b013e318189f13c. PMID:19307989

18. Facciabene A, Motz GT, Coukos G. T-regulatory cells: key players in tumor immune escape and angiogenesis. Cancer Res. 2012;72:2162–71. doi:10.1158/0008-5472.CAN-11-3687. PMID:22549946

19. Shang B, Liu Y, Jiang SJ, Liu Y. Prognostic value of tumor-infiltrating FoxP3+ regulatory T cells in cancers: a systematic review and meta-analysis. Sci Rep. 2015;5:15179. doi:10.1038/srep15179. PMID:26462617

20. Bacman D, Merkel S, Croner R, Papadopoulos T, Brueckl W, Dimmler A. TGF-beta receptor 2 downregulation in tumour-associated stroma worsens prognosis and high-grade tumours show more tumour-associated macrophages and lower TGF-beta1 expression in colon carcinoma: a retrospective study. BMC Cancer. 2007;7:156. doi:10.1186/1471-2407-7-156. PMID:17692120

21. Hawinkels LJ, Verspaget HW, van Duijn W, van der Zon JM, Zuidwijk K, Kubben FJ, Verheijen JH, Hommes DW, Lamers CB, Sier CF. Tissue level, activation and cellular localisation of TGF-beta1 and association with survival in gastric cancer patients. Br J Cancer. 2007;97:398–404. doi:10.1038/sj.bjc.6603877. PMID:17637685

22. Kim IY, Ahn HJ, Lang S, Oefelein MG, Oyasu R, Kozlowski JM, Lee C. Loss of expression of transforming growth factor-beta receptors is associated with poor prognosis in prostate cancer patients. Clin Cancer Res 1998;4:1625–30. PMID:9676836

23. Akhurst RJ. Targeting TGF-beta signaling for therapeutic gain. Cold Spring Harb Perspect Biol. 2017;9. doi:10.1101/cshperspect.a022301. PMID:28246179

24. Yingling JM, Blanchard KL, Sawyer JS. Development of TGF-beta signalling inhibitors for cancer therapy. Nat Rev Drug Discov. 2004;3:1011–22. doi:10.1038/nrd1580. PMID:15573100

25. Lan Y. Preclinical evaluation of M7824 (MSB0011359 C), a novel bifunctional fusion protein targeting the PD-L1 and TGFb pathways. Keystone Symposia on Molecular and Cellular Biology, Taos, NM, Jan. 9–13, 2017.

26. Massagué J. TGFβ in cancer. Cell. 2008;134:215–30. doi:10.1016/j.cell.2008.07.001. PMID:18662538

27. Pardoll DM. The blockade of immune checkpoints in cancer immunotherapy. Nat Rev Cancer. 2012;12:252–64. doi:10.1038/nrc3239. PMID:22437870

28. Sanjabi S, Oh SA, Li MO. Regulation of the immune response by TGF-beta: from conception to autoimmunity and infection. Cold Spring Harb Perspect Biol. 2017;9: a022236. doi:10.1101/cshperspect.a022236. PMID:28108486

29. Strauss J, Heery CR, Schlom J, Madan RA, Cao L, Kang Z, et al. Phase 1 trial of M7824 (MSB0011359 C), a bifunctional fusion protein targetingPD-L1 and TGF-β, in advanced solid tumors. Clin Cancer Res. 2018. pii: clincanres.2653.2017. doi:10.1158/1078-0432.CCR-17-2653. [Epub ahead of print].

30. Yu P, Lee Y, Liu W, Krausz T, Chong A, Schreiber H, Fu YX. Intratumor depletion of CD4+ cells unmasks tumor immunogenicity leading to the rejection of late-stage tumors. J Exp Med. 2005;201:779–91. doi:10.1084/jem.20041684. PMID:15753211

31. Andre MC, Sigurdardottir D, Kuttruff S, Pommerl B, Handgretinger R, Rammensee HG, Steinle A. Impaired tumor rejection by memory CD8 T cells in mice with NKG2D dysfunction. Int J Cancer. 2012;131:1601–10. doi:10.1002/ijc.26191. PMID:21607945

32. Hu J, Zhu S, Xia X, Zhang L, Kleinerman ES, Li S. CD8+T cell-specific induction of NKG2D receptor by doxorubicin plus interleukin-12 and its contribution to CD8+T cell accumulation in tumors. Mol Cancer. 2014;13:34. doi:10.1186/1476-4598-13-34. PMID:24565056

33. McAdam AJ, Felcher A, Woods ML, Pulaski BA, Hutter EK, Frelinger JG, Lord EM. Transfection of transforming growth factor-beta producing tumor EMT6 with interleukin-2 elicits tumor rejection and tumor reactive cytotoxic T-lymphocytes. J Immunother Emphasis Tumor Immunol 1994;15:155–64. doi:10.1097/00002371-199404000-00001. PMID:8032538

34. Pickup M, Novitskiy S, Moses HL. The roles of TGFβ in the tumour microenvironment. Nat Rev Cancer. 2013;13:788–99. doi:10.1038/nrc3603. PMID:24132110

35. Je EC, Lca BS, Ga GA. The role of transcription factor TWIST in cancer cells. J Genet Syndr Gene Ther. 2013;4:124.

36. Puisieux A, Valsesia-Wittmann S, Ansieau S. A twist for survival and cancer progression. Br J Cancer. 2006;94:13–7. doi:10.1038/sj.bjc.6602876. PMID:16306876

37. Ardiani A, Gameiro SR, Palena C, Hamilton DH, Kwilas A, King TH, Schlom J, Hodge JW. Vaccine-mediated immunotherapy directed against a transcription factor driving the metastatic process. Cancer Res. 2014;74:1945–57. doi:10.1158/0008-5472.CAN-13-2045. PMID:24520078

38. Kwilas AR, Ardiani A, Dirmeier U, Wottawah C, Schlom J, Hodge JW. A poxviral-based cancer vaccine the transcription factor twist inhibits primary tumor growth and metastases in a model of metastatic breast cancer and improves survival in a spontaneous prostate cancer model. Oncotarget. 2015;6:28194–210. doi:10.18632/oncotarget.4442. PMID:26317648

39. Terabe M, Robertson FC, Clark K, De Ravin E, Bloom A, Venzon DJ, Kato S, Mirza A, Berzofsky JA. Blockade of only TGF-beta 1 and 2 is sufficient to enhance the efficacy of vaccine and PD-1 checkpoint blockade immunotherapy. Oncoimmunology. 2017;6:e1308616. doi:10.1080/2162402X.2017.1308616. PMID:28638730

40. Jochems C, Tritsch SR, Pellom ST, Su Z, Soon-Shiong P, Wong HC, Gulley JL, Schlom J. Analyses of functions of an anti-PD-L1/TGFbetaR2 bispecific fusion protein (M7824). Oncotarget. 2017;8:75217–31. PMID:29088859

41. Bierie B, Moses HL. Tumour microenvironment: TGFbeta: the molecular Jekyll and Hyde of cancer. Nat Rev Cancer. 2006;6:506–20. doi:10.1038/nrc1926. PMID:16794634

42. Kretschmer A, Moepert K, Dames S, Sternberger M, Kaufmann J, Klippel A. Differential regulation of TGF-beta signaling through Smad2, Smad3 and Smad4. Oncogene. 2003;22:6748–63. doi:10.1038/sj.onc.1206791. PMID:14555988

43. Liu L, Liu X, Ren X, Tian Y, Chen Z, Xu X, Du Y, Jiang C, Fang Y, Liu Z, et al. Smad2 and Smad3 have differential sensitivity in relaying TGFβ signaling and inversely regulate early lineage specification. Scientific Reports. 2016;6:21602. doi:10.1038/srep21602. PMID:26905010

44. Ungefroren H, Groth S, Sebens S, Lehnert H, Gieseler F, Fandrich F. Differential roles of Smad2 and Smad3 in the regulation of TGF-beta1-mediated growth inhibition and cell migration in pancreatic ductal adenocarcinoma cells: control by Rac1. Mol Cancer. 2011;10:67. doi:10.1186/1476-4598-10-67. PMID:21624123

45. David JM, Dominguez C, McCampbell KK, Gulley JL, Schlom J, Palena C. A novel bifunctional anti-PD-L1/TGF-beta Trap fusion protein (M7824) efficiently reverts mesenchymalization of human lung cancer cells. Oncoimmunology. 2017;6:e1349589. doi:10.1080/2162402X.2017.1349589. PMID:29123964

46. Henriksen R, Gobl A, Wilander E, Oberg K, Miyazono K, Funa K. Expression and prognostic significance of TGF-beta isotypes, latent TGF-beta 1 binding protein, TGF-beta type I and type II receptors, and endoglin in normal ovary and ovarian neoplasms. Lab Invest 1995;73:213–20. PMID:7637321

47. Bierie B, Moses HL. Gain or loss of TGF-β signaling in mammary carcinoma cells can promote metastasis. Cell Cycle. 2009;8:3319–27. doi:10.4161/cc.8.20.9727. PMID:19806012

48. Castriconi R, Cantoni C, Della Chiesa M, Vitale M, Marcenaro E, Conte R, Biassoni R, Bottino C, Moretta L, Moretta A. Transforming growth factor beta 1 inhibits expression of NKp30 and NKG2D receptors: consequences for the NK-mediated killing of dendritic cells. Proc Natl Acad Sci U S A. 2003;100:4120–5. doi:10.1073/pnas.0730640100. PMID:12646700

49. Freeman GJ, Long AJ, Iwai Y, Bourque K, Chernova T, Nishimura H, Fitz LJ, Malenkovich N, Okazaki T, Byrne MC, et al. Engagement of the PD-1 immunoinhibitory receptor by a novel B7 family member leads to negative regulation of lymphocyte activation. J Exp Med. 2000;192:1027–34. doi:10.1084/jem.192.7.1027. PMID:11015443

50. Thomas DA, Massague J. TGF-beta directly targets cytotoxic T cell functions during tumor evasion of immune surveillance. Cancer Cell. 2005;8:369–80. doi:10.1016/j.ccr.2005.10.012. PMID:16286245

51. Beldi-Ferchiou A, Lambert M, Dogniaux S, Vely F, Vivier E, Olive D, Dupuy S, Levasseur F, Zucman D, Lebbé C, et al. PD-1 mediates

functional exhaustion of activated NK cells in patients with Kaposi sarcoma. Oncotarget. 2016;7:72961–77. PMID:27662664

52. Selenko-Gebauer N, Majdic O, Szekeres A, Hofler G, Guthann E, Korthauer U, Zlabinger G, Steinberger P, Pickl WF, Stockinger H, et al. B7-H1 (programmed death-1 ligand) on dendritic cells is involved in the induction and maintenance of T cell anergy. J Immunol. 2003;170:3637–44. doi:10.4049/jimmunol.170.7.3637. PMID:12646628

53. Pauken KE, Wherry EJ. Overcoming T cell exhaustion in infection and cancer. Trends Immunol. 2015;36:265–76. doi:10.1016/j.it.2015.02.008. PMID:25797516

54. Zhang N, Bevan MJ. TGF-beta signaling to T cells inhibits autoimmunity during lymphopenia-driven proliferation. Nat Immunol. 2012;13:667–73. doi:10.1038/ni.2319. PMID:22634866

55. Cha E, Klinger M, Hou Y, Cummings C, Ribas A, Faham M, Fong L. Improved survival with T cell clonotype stability after anti-CTLA-4 treatment in cancer patients. Sci Transl Med. 2014;6:238ra70. doi:10.1126/scitranslmed.3008211. PMID:24871131

56. McNeel DG. TCR diversity – a universal cancer immunotherapy biomarker? J Immunother Cancer. 2016;4:69. doi:10.1186/s40425-016-0175-4. PMID:27879971

57. Postow MA, Manuel M, Wong P, Yuan J, Dong Z, Liu C, Perez S, Tanneau I, Noel M, Courtier A, et al. Peripheral T cell receptor diversity is associated with clinical outcomes following ipilimumab treatment in metastatic melanoma. J Immunother Cancer. 2015;3:23. doi:10.1186/s40425-015-0070-4. PMID:26085931

58. Gulley JL, Madan RA, Tsang KY, Jochems C, Marte JL, Farsaci B, Tucker JA, Hodge JW, Liewehr DJ, Steinberg SM, et al. Immune impact induced by PROSTVAC (PSA-TRICOM), a therapeutic vaccine for prostate cancer. Cancer Immunol Res. 2014;2:133–41. doi:10.1158/2326-6066.CIR-13-0108. PMID:24778277

59. Kudo-Saito C, Schlom J, Hodge JW. Induction of an antigen cascade by diversified subcutaneous/intratumoral vaccination is associated with antitumor responses. Clin Cancer Res. 2005;11:2416–26. doi:10.1158/1078-0432.CCR-04-1380. PMID:15788693

60. Robbins PF, Kantor JA, Salgaller M, Hand PH, Fernsten PD, Schlom J. Transduction and expression of the human carcinoembryonic antigen gene in a murine colon carcinoma cell line. Cancer Res 1991;51:3657–62. PMID:1712245

61. Pulaski BA, Ostrand-Rosenberg S. Mouse 4T1 breast tumor model. Curr Protoc Immunol. 2001;Chapter 20:Unit 20.2. doi:10.1002/0471142735.im2002s39. PMID:18432775

62. Flanders KC, Yang YA, Herrmann M, Chen J, Mendoza N, Mirza AM, Wakefield LM. Quantitation of TGF-beta proteins in mouse tissues shows reciprocal changes in TGF-beta1 and TGF-beta3 in normal vs neoplastic mammary epithelium. Oncotarget. 2016;7:38164–79. doi:10.18632/oncotarget.9416. PMID:27203217

63. Kopp JB, Factor VM, Mozes M, Nagy P, Sanderson N, Bottinger EP, Klotman PE, Thorgeirsson SS. Transgenic mice with increased plasma levels of TGF-beta 1 develop progressive renal disease. Lab Invest. 1996;74:991–1003. PMID:8667617

64. Chen JQ, Heldman MR, Herrmann MA, Kedei N, Woo W, Blumberg PM, Goldsmith PK. Absolute quantitation of endogenous proteins with precision and accuracy using a capillary Western system. Anal Biochem. 2013;442:97–103. doi:10.1016/j.ab.2013.07.022. PMID:23896461